Separation Science and Technology
Publication details, including instructions for authors and subscription information:
http://www.informaworld.com/smpp/title~content=t713708471

Multi-Isotope Separation in a Gas Centrifuge Using Onsager's Pancake Model

Houston G. Wood[a]; Thomas C. Mason[a]; Soubbaramayer[a]
[a] DEPARTMENT OF MECHANICAL, AEROSPACE & NUCLEAR ENGINEERING, UNIVERSITY OF VIRGINIA, CHARLOTTESVILLE, VIRGINIA, USA

To cite this Article Wood, Houston G. , Mason, Thomas C. and Soubbaramayer(1996) 'Multi-Isotope Separation in a Gas Centrifuge Using Onsager's Pancake Model', Separation Science and Technology, 31: 9, 1185 — 1213
To link to this Article: DOI: 10.1080/01496399608006946
URL: http://dx.doi.org/10.1080/01496399608006946

SEPARATION SCIENCE AND TECHNOLOGY, 31(9), pp. 1185–1213, 1996

Multi-Isotope Separation in a Gas Centrifuge Using Onsager's Pancake Model

HOUSTON G. WOOD, THOMAS C. MASON,
and SOUBBARAMAYER
DEPARTMENT OF MECHANICAL, AEROSPACE & NUCLEAR ENGINEERING
UNIVERSITY OF VIRGINIA
CHARLOTTESVILLE, VIRGINIA 22903, USA

ABSTRACT

A method is developed to compute the optimal multi-isotope separation in a gas centrifuge. The method relies on three models: Onsager's pancake equation, diffusion equations written for each isotope, and an optimization routine. Onsager's equation, well studied in the past for UF_6, is adapted to multi-isotope gas mixtures, focusing on the three drives generating the countercurrent flow in practical centrifuges: feed drive, scoop drive, and linear wall thermal drive. Diffusion equations are written for each isotope in the initial form of partial differential equations (PDE) and reduced to ordinary differential equations (ODE) by the radial averaging method. These ODEs, linked with the solution of Onsager's equation through two parameters (flow profile efficiency and scaled countercurrent flow), are solved by an iteration method. The optimization routine is based on a choice of a strategy and a method, using the solutions of the two preceeding models, to determine the optimal countercurrent driving parameters. Two examples of application, having an industrial interest respectively in the reprocessing of nuclear waste and in the production of stable isotopes, are presented: The reenrichment of spent reactor uranium and the separation of chromium isotopes.

1. INTRODUCTION

Over the past years, several countries have funded important programs to develop and deploy gas centrifuges for enriching uranium in the fissionable isotope U-235. As a result, the centrifugation process has reached full industrial maturity and several large-scale production plants are now operating in different countries such as Germany, Holland, Great Britain

(the three partners in Urenco), Russia, and Japan. The total enrichment capacity of those centrifuge plants presently represents about one-third of the world enrichment capacity, making centrifugation the second most used industrial process after gaseous diffusion. The position of the United States has evolved somewhat differently. The US Department of Energy (DOE) spent 25 years developing the gas centrifuge process and increased, according to Roberts (1), the separative performance of the unitary machine from less than one separative work unit (swu) for a centrifuge with a rotor of 7.6 cm diameter and 38.1 cm long to 200 swu's for a centrifuge with a rotor of 0.61 m diameter and 12.2 m long. A separative work unit is about the separative capacity required to produce 0.25 kg/yr of 3% U-235 reactor-grade fuel from natural 0.7% U-235 while stripping the tails materials to 0.2% U-235. Nevertheless, in 1985 the DOE shut down in 1985 its centrifuge program because of a plateau in both domestic and world demand for nuclear fuel. At the same time, the United States also made the decision to meet its near-term need for enriched uranium with the existing gaseous diffusion plants and to continue the development work on the Atomic Vapor Laser Isotope Separation (AVLIS) process to meet 21st century needs.

More recently, some interest has appeared for using existing gas centrifuges to separate other isotopes like stable isotopes or spent reactor uranium isotopes. The motivations of that interest are different. There is a growing demand in medicine and fundamental physics research laboratories for stable isotopes. The use of the gas centrifugation process makes it possible to produce isotopes of several elements when large (kilogram) quantities are commercially needed. For instance, this is the case for xenon, krypton, tungsten, molybdenum, rhenium, iridium, tellurium, sulfur, germanium, chromium, and others. Regarding spent reactor uranium, the problem was raised in some countries in the framework of the nuclear waste reprocessing cycle. Once all the radioactive elements are removed, the remaining spent reactor uranium contains five isotopes, U-232, U-234, U-235, U-236, and U-238. The concentration of the fissionable U-235 is about 1%, much higher than the 0.71% concentration of U-235 in natural uranium. In a sense, once the stock of spent reactor uranium is reprocessed, it is a uranium mine richer than any natural mine. The idea is to reenrich that spent reactor uranium and use it again as fuel for power reactors, thus closing the reprocessing cycle. A number of papers can be found in the public literature reporting on this type of separation activities by gas centrifuge in the USA (1, 2) China (3), Russia (4–6), and Urenco (7). It is obvious that a centrifuge designed for the production of fuel for nuclear reactors cannot separate with equal efficiency other isotopic mixtures for which the molecular mass is quite different and for which the number of components is much more than two. A conversion

of existing facilities is necessary and requires a reoptimization of working parameters according to each specific process gas. The goal of the present paper is to adapt the theoretical models that supported the uranium centrifuge program to the multi-isotope mixtures and to reoptimize, with a new optimization strategy, the countercurrent driving parameters like the scoop drag, the linear wall temperature gradient, the feed rate, and the cut. Our investigation is restricted to a single centrifuge. The problem of cascading for multi-isotope separation is not dealt with in this paper (the reader is referred to Refs. 8–13).

The model describing the phenomena in a centrifuge includes a set of equations describing the fluid dynamics of the countercurrent and the diffusion equations written for each isotope of the mixture. The problem is solved in two steps. In the first step, described in Section 2, the gas dynamics is solved for an average mass velocity, density, and temperature of the mixture as a whole. We use Onsager's pancake model with internal source/sink terms. Solution of this model has been investigated by Wood et al. (14–16). The introduction of the feed gas plays an important role in establishing the countercurrent flow. We use one of the three models developed by Wood (17). In the second step, the solution found in the first step for the countercurrent flow is employed for solving the diffusion equations. In Section 3 we start by writing the set of nonlinear partial differential equations (PDEs) governing the diffusion-convection of each isotope, and then we give the reduction of the PDEs to a set of nonlinear ordinary differential equations (ODEs) by the method of radial averaging (18–21). The solution of the countercurrent flow of Section 2 is introduced in these ODEs through two functions: flow profile efficiency e_F and normalized countercurrent flow m, both being functions of the axial coordinate. We terminate Section 3 by giving the solution of the ODEs by the method of iteration developed by Harink-Snijders (22). However, the latter author has not proceeded to the optimization of the countercurrent driving parameters. In Section 4 we define a new optimization strategy for multi-isotope mixtures, as the classical quantities like value function and separative power, which are so fundamental in the case of binary isotopic mixtures, are no more available in multi-isotope cases. Section 4 culminates in two examples of practical calculation of optimal centrifuge parameters for the reenrichment of spent reactor uranium and for the separation of stable isotopes of chromium.

2. FLUID DYNAMICS OF A GAS CENTRIFUGE

The fluid dynamics model used in this study is the Onsager pancake equation with the inclusion of internal source/sink terms (14–16). This is summarized in Section 2.1. The introduction of the feed gas plays an

important role in establishing the secondary countercurrent flow, and Wood has developed a feed model to study the effects of the feed flow on the separation of a single-stage gas centrifuge cascade. The feed model used by Wood (17) is described in Section 2.2.

2.1. Onsager Pancake Model with Source/Sink Terms

The derivation of the equations has been reported in numerous articles by Wood et al. In this model the solution to the equations of motion for a viscous heat-conducting compressible ideal fluid is assumed to be representable as a perturbation about solid body isothermal flow in a right circular cylinder. The perturbation equations can be combined into a single sixth-order, linear partial differential equation

$$(e^x(e^x\chi_{xx})_{xx})_{xx} + B^2\chi_{yy} = F(x, y) \tag{2.1}$$

where χ is a master potential from which the physical variables can be extracted. The independent variable

$$x = A^2\left[1 - \left(\frac{r}{a}\right)^2\right]$$

is the radial scale height or e-folding distance for the density and y is the axial variable scaled by the radius, a, of the cylinder. The variable $B^2 = \mathrm{Re}^2 S/16A^{12}$ is a parameter containing the physical description of the particular rotor and operating parameters. In particular, $\mathrm{Re} = \rho_w \Omega a^2/\mu$ where ρ_w is the density at the wall, Ω is the frequency of rotation, and μ is the viscosity where the bulk viscosity has been taken to be 0. The quantity $S = 1 + \mathrm{Pr}A^2(\gamma - 1)/2\gamma$ is a thermodynamic variable where γ is the ratio of specific heats and Pr is the Prandtl number. The speed parameter is $A^2 = \Omega^2 a^2/2RT_0$, where T_0 is the average temperature of the gas and R is the specific gas constant. The nonhomogeneous term $F(x, y)$ arises from internal sources or sinks of mass, momentum, or energy and is written

$$\begin{aligned} F(x, y) = {} & \frac{B^2A^2}{2\mathrm{Re}S}\int_x^{x_T}(Z_y - 2V_y)dx' - \frac{B^2}{2\mathrm{Re}S}\int_x^{x_T} \\ & \times \int_0^{x'}(Z_y + 2(S - 1)\,V_y)dx'dx'' - \frac{B^2}{4A^4}\int_x^{x_T} \\ & \times \int_0^{x'} M_y dx'dx'' - \frac{B^2A^2}{2\mathrm{Re}S}[(e^xU_y)_x + (e^xW)_{xx}] \end{aligned} \tag{2.2}$$

Here M, U, V, W, and Z are dimensionless quantities which represent

source terms in the modified forms of the conservation equations for mass, momentum, and energy. In terms of the dimensional physical variables, the source of mass is M, the source of momentum is $\mathbf{F}_s = (F_r, F_\theta, F_z)$, and sources of heat and work are Q and W. The mass introduced by the source has temperature T_s, velocity $\mathbf{V}_s = (V_r, V_\theta, V_z)$, and the local velocity of the rotating gas is assumed to be given by solid body rotation or $\mathbf{q} = (0, \Omega r, 0)$. The quantities in Eq. (2.2) are related to these physical variables as follows:

$$M = \mathrm{M}/\rho_w\Omega \tag{2.3a}$$

$$U = (\mathrm{M}v_r + F_r)/\rho_w\Omega^2 a \tag{2.3b}$$

$$V = (\mathrm{Re}/4A^4)\,[(v_\theta - \Omega r)\mathrm{M} + F_\theta]/\rho_w\Omega^2 a \tag{2.3c}$$

$$W = 2A^2[\mathrm{M}v_z + F_z]/\rho_w\Omega^2 a \tag{2.3d}$$

$$Z = \frac{1}{4A^4}\left\{Q + W - q\cdot F_s + M\left[\frac{(V_s - q)^2}{2} - c_p(T_0 - T_s)\right]\right\}/(kT_0/a^2) \tag{2.3e}$$

2.2. A Feed Model

At high rates of rotation, the gas is compressed into a narrow annular region near the cylinder wall and a very good vacuum is established in the center region of the centrifuge. The feed gas is introduced from a hole in the pipe which is located along the axis of rotation (see Fig. 1). We assume the stagnation conditions in the feed reservoir are known, and that the hole is a choked orifice. This allows the velocity and temperature of the expanded gas to be determined. Further, this expanded gas is frozen in all of its modes except the transnational mode. Therefore, the gas continues with this temperature along the trajectory until it reaches the denser region and collides with the rotating gas. We assume that this collision occurs at a radial position where the mean free path is equal to a local density scale height, and that with one collision the feed gas is accelerated to rotational speed. We assume the expansion from stagnation conditions T_0, $V_0 \simeq 0$ to T_s, V_s is adiabatic so that $c_p(T_0 - T_s) = \frac{1}{2}V_s^2$ which is substituted into Eq. (2.3e). Therefore the source terms which model the introduction of feed are

$$M = \mathrm{M}/\rho_w\Omega \tag{2.4a}$$

$$U = \mathrm{M}v_r/\rho_w\Omega^2 a \tag{2.4b}$$

$$V = (\mathrm{Re}/4A^4)\,(v_\theta - \Omega r)\mathrm{M}/\rho_w\Omega^2 a \tag{2.4c}$$

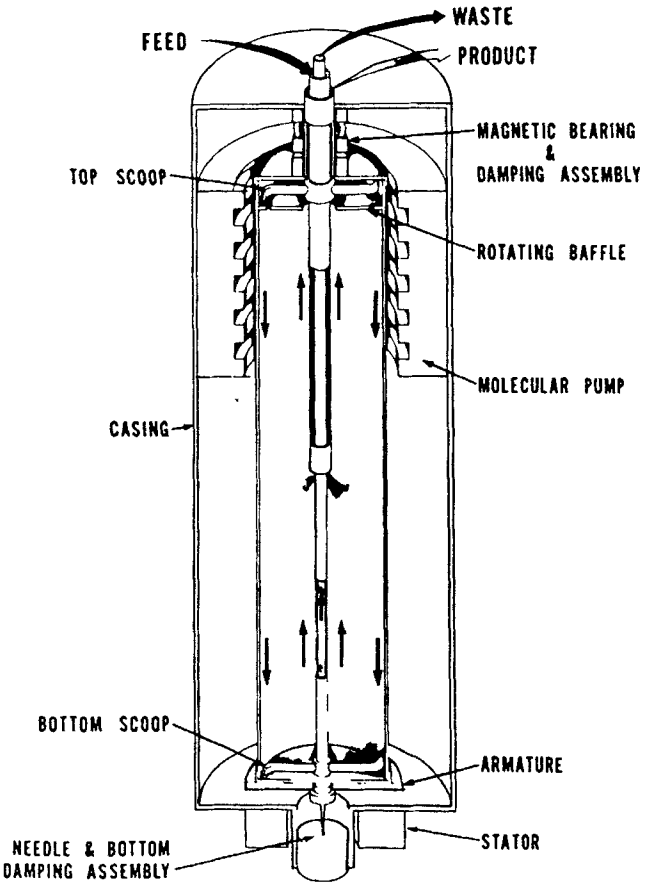

FIG. 1 Schematic of a gas centrifuge.

$$W = 2A^2 M v_z/\rho_w \Omega^2 a \tag{2.4d}$$

$$Z = (a/4A^4)M^{1/2}[(V_s - q)^2 - V_s^2]/(kT_0/a^2) \tag{2.4e}$$

In Eqs. (2.4) the mass is assumed to enter by the formula

$$M = M_0 \delta(x - x^*)G(y)$$

where

$$G(y) = \begin{cases} 0 & 0 \le y < y^* - 1.5 \\ 1 & y^* - 1.5 \le y \le y^* + 1.5 \\ 0 & y^* + 1.5 < y \le y_T \end{cases}$$

where $y^* = y_T/2$, and δ is the Dirac delta function. This implies that the mass enters in a ring of axial extent equal to 3 radii centered about the midplane. For the source velocity $\mathbf{V} = (v_r, v_\theta, v_z)$, we choose $v_z = 0$ and $v_r = (\gamma RT_0)^{1/2}$, sound speed for the gas. This simulates the case of choked flow through the orifice in the center post. The azimuthal component of the source velocity is taken to be equal to the local velocity of solid body rotation. This assumes the feed flow has been spun up so that $v_\theta = \Omega r^*$.

The conditions of no shear and no heat flux are imposed on Eq. (2.1) at the inner boundary or top of the atmosphere at a radial location $x = x_T$, where x_T is chosen large enough so that the solution is independent of the choice. Numerical experiments have shown that $x_T = 15$ is large enough, and this value is generally used. This is consistent with the analysis of this problem by Cooper and Morton (23). The radial location of the feed gas collision depends on operating parameters such as the rotation rate and inventory, and for the cases considered ranges from approximately $x = 8$ to $x = 10$. Because of the assumptions regarding the feed, the boundary conditions at $x = x_T$ are *not* changed. The relationship between the different radial locations is displayed in Fig. 2.

The mass that is introduced by the feed can be removed through a boundary or a sink. Again referring to Fig. 1 with an upper baffle, a model of this geometric configuration would allow for mass removal through the upper boundary and through a sink located at the position corresponding to the bottom scoop. This scoop is stationary and acts as a sink of angular

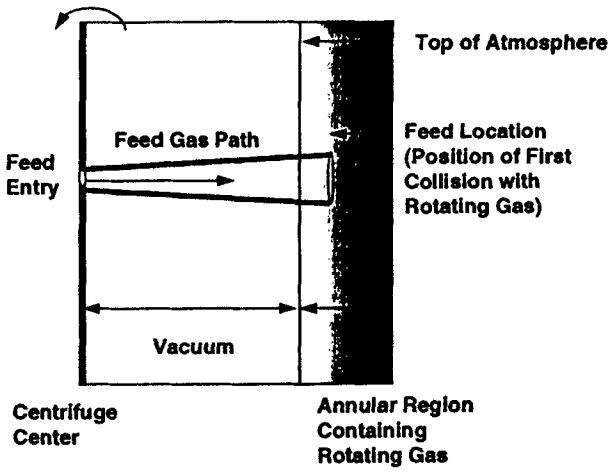

FIG. 2 Schematic of the feed model.

momentum or a source of drag. Therefore, $\mathbf{F}_s = (0, F_\theta, 0)$, where F_θ is the drag force exerted by the scoop, and $\mathbf{q}\cdot\mathbf{F}_s = \Omega r^* F_\theta$ is the scoop drag power. The source model for the scoop drag is then

$$M = U = W = 0 \tag{2.5a}$$

$$V = (\mathrm{Re}/4A^4)F_\theta/\rho_w\Omega^2 a \tag{2.5b}$$

$$Z = -(1/4A^4)\Omega r^* F_\theta/(kT_0/a^2) \tag{2.5c}$$

Here, F_θ is negative since the scoop is a sink of angular momentum. If the valve is closed so that no mass is removed by the scoop, Eq. (2.5) models the action of the scoop on the gas.

In the case where mass is removed by the scoop, the source terms will be the sum of those given by Eqs. (2.4) and (2.5) with M taken as negative to reflect a sink of mass. If the control volume used is taken in front of the scoop, the gas can be assumed to leave the system with the velocity of solid body rotation so that $\mathbf{V}_s = (0, \Omega r^*, 0)$. For example, we see that Eq. (2.4e) is simply

$$Z = -(1/4A^4)\mathrm{M}^{1/2}(\Omega r^*)^2/(kT_0/a^2) \tag{2.6}$$

which represents the kinetic energy of the gas leaving the system.

3. SEPARATION EQUATIONS FOR A MULTI-ISOTOPE MIXTURE AND SOLUTION

For a mixture of n isotopes, the separation is basically governed by a set of n diffusion equations with appropriate boundary conditions (Section 3.1). These equations are nonlinear two-dimensional partial differential equations (PDEs) and are not easily tractable. The radial averaging method (Section 3.2) reduces the set of PDEs into a set of ordinary differential equations (ODEs) much easier to solve. This set of ODEs is expressed (Section 3.3) in terms of Onsager's master potential and solved (Section 3.4) by the iteration method.

3.1. Diffusion Equations

The net transport vector $\vec{\phi}_k$ of isotope k in the centrifuge is the balance between three basic transport phenomena depicted in Fig. 3: pressure diffusion $\vec{\phi}_k^P$ (thin arrow), backdiffusion $\vec{\phi}_k^B$ (medium weight arrow), and convection $\vec{\phi}_k^C$ (thick arrow):

$$\vec{\phi}_k = \vec{\phi}_k^P + \vec{\phi}_k^B + \vec{\phi}_k^C \tag{3.1}$$

The first one is the primary separative effect by centrifugation, while the

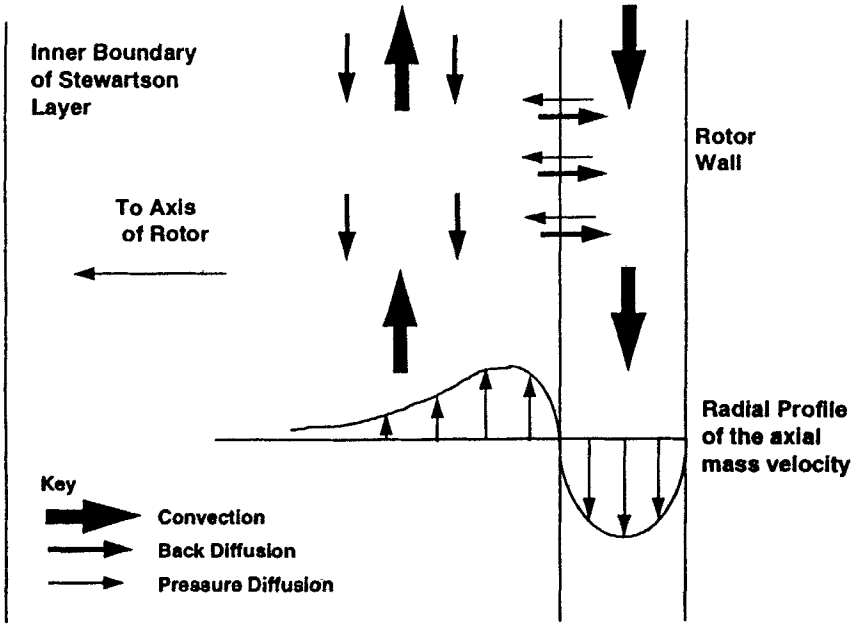

FIG. 3 Schematic of the three basic transport phenomena acting on each isotope in the centrifuge.

two others are separation efficiency decreasing factors. The radial and axial components of the three basic transports follow:

$$\vec{\phi}_k^P \left(\frac{DM_k}{RT} \frac{\partial P_k}{\partial r}, 0 \right) \tag{3.2a}$$

$$\vec{\phi}_k^B \left(-D \frac{\partial \rho_k}{\partial r}, -D \frac{\partial \rho_k}{\partial z} \right) \tag{3.2b}$$

$$\vec{\phi}_k^C (\rho_k V_r, \rho_k V_z) \tag{3.2c}$$

The gas is assumed to be perfect and to behave isothermally. The mass density ρ_k is related to the mole fraction N_k and to the total mass density ρ by

$$\rho = \sum_{j=1}^{n} \rho_j \qquad \rho_k = \rho N_k \qquad \sum_{j=1}^{n} N_j = 1 \tag{3.3}$$

We recall the pressure diffusion relation to the centrifugal acceleration

$$\frac{\partial P_k}{\partial r} = \rho_k \Omega^2 r \; (= \rho \Omega^2 r N_k) \tag{3.4}$$

Substituting Eqs. (3.3) and (3.4) into Eq. (3.2) results in the following expressions for the three transports:

$$\vec{\phi}_k^{\,p} \left(\rho D \frac{\Omega^2 r}{RT} M_k N_k, \; 0 \right) \tag{3.5a}$$

$$\vec{\phi}_k^{\,B} \left(-\rho D \frac{\partial N_k}{\partial r} - \rho D \frac{\Omega^2 r}{RT} N_k \sum_{j=1}^{n} M_j N_j, \; -\rho D \frac{\partial N_k}{\partial z} \right) \tag{3.5b}$$

$$\vec{\phi}_k^{\,c} (\rho V_r N_k, \; \rho V_z N_k) \tag{3.5c}$$

The radial component $\phi_{k,r}$ and the axial component $\phi_{k,z}$ of the net transport vector $\vec{\phi}_k$ are easily derived by substituting Eq. (3.5) into Eq. (3.1):

$$\phi_{k,r} = \rho D \frac{\Omega^2 r}{RT} M_k N_k - \rho D \frac{\partial N_k}{\partial r} - \rho D \frac{\Omega^2 r}{RT} N_k \sum_{j=1}^{n} M_j N_j + \rho V_r N_k \tag{3.6a}$$

$$\phi_{k,z} = -\rho D \frac{\partial N_k}{\partial z} + \rho V_z N_k \tag{3.6b}$$

The steady-state conservation law for isotope k in the centrifuge is

$$\operatorname{div} \vec{\phi}_k = \frac{1}{r} \frac{\partial}{\partial r} (r \phi_{k,r}) + \frac{\partial}{\partial Z} \phi_{k,z} = 0 \tag{3.7}$$

Assuming that (ρD) is constant and introducing Eq. (3.6) in Eq. (3.7) results in the diffusion equation for isotope k:

$$-\rho D \frac{\partial^2 N_k}{\partial Z^2} - \rho D \frac{1}{r} \frac{\partial}{\partial r} \left[r \frac{\partial N_k}{\partial r} - \frac{\Omega^2 r^2}{RT} \left(M_k - \sum_{j=1}^{n} M_j N_j \right) N_k \right] + \rho V_z \frac{\partial N_k}{\partial Z} = 0 \tag{3.8}$$

Equation (3.8) is derived by using the continuity equation of fluid dynamics and by neglecting the radial convection term $\rho V_r (\partial N_k / \partial r)$. The latter assumption is justified by the fact that the radial component V_r of the velocity is predominant over the axial component V_z only in the very thin Ekman layers, i.e., very near the end caps.

Equation (3.8) should be completed by appropriate boundary conditions as follows:

- There is no radial transport at the rotor wall and on the axis:

$$\text{at} \quad r = a: \qquad \frac{\partial N_k}{\partial r} - \frac{\Omega^2 a}{RT}\left(M_k - \sum_{j=1}^{n} M_j N_j\right) N_k = 0 \tag{3.9}$$

$$\text{at} \quad r = 0: \qquad \frac{\partial N_k}{\partial r} = 0 \tag{3.10}$$

- The axial transport over the end caps equals a constant. The value of the constant is different according to the end cap, as it takes into account the removal of the enriched and depleted streams from the centrifuge (Fig. 4).

$$\text{at} \quad z = 0: \qquad \int_0^a \phi_{k,z} 2\pi r dr = \int_0^a \left(-\rho D \frac{\partial N_k}{\partial Z} + \rho V_z N_k\right) 2\pi r dr = -F(1 - \theta) N_{w,k} \tag{3.11}$$

$$\text{at} \quad z = z_H: \qquad \int_0^a \phi_{k,z} 2\pi r dr = \int_0^a \left(-\rho D \frac{\partial N_k}{\partial Z} + \rho V_z N_k\right) 2\pi r dr = F\theta N_{p,k} \tag{3.12}$$

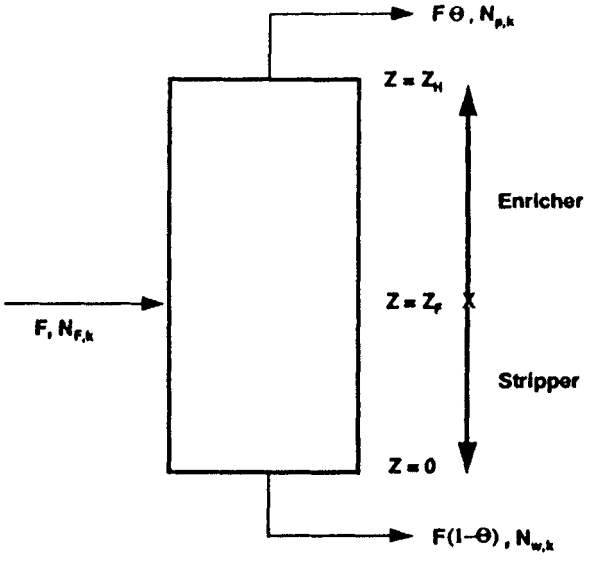

FIG. 4 Schematic of a centrifuge with one feed port and two extractors at the extreme ends of the rotor.

Finally, it should be noted that the feed concentration $N_{F,k}$ is related to $N_{p,k}$ and $N_{w,k}$ by the overall balance equation for the isotope k:

$$N_{F,k} = \theta N_{p,k} + (1 - \theta)N_{w,k} \tag{3.13}$$

For a mixture of n isotopes, n equations like Eq. (3.8) together with n sets of boundary conditions similar to the set of Eqs. (3.9)–(3.13) are to be solved. We recall that in Eq. (3.8) the axial mass velocity field $\rho V_z(r, z)$ should come out from the solution of Onsager's pancake model.

3.2. Radial Averaging Approximation

The above-mentioned set of diffusion equations are nonlinear, two-dimensional, partial differential equations and are too complex to be solved directly by mathematical methods or even by computational facilities. A very good approximation can be obtained by the radial averaging method which reduces the (r, z) dimensional PDEs to z dimensional ordinary differential equations. The method consists in seeking the solution for the radially averaged mole fraction of isotope k

$$\overline{N}_k = \frac{1}{\pi a^2} \int_0^a N_k 2\pi r dr \tag{3.14}$$

The new variable $\overline{N}_k$ depends only on the axial coordinate z. The way we follow is quite similar to the one in the case of a binary mixture. We start from the steady-state conservation law Eq. (3.7), multiply the two sides by $2\pi r dr$, and integrate from $r = 0$ to $r = a$. We have, by taking into account the boundary conditions (3.9) and (3.10):

$$\int_0^a \phi_{k,z}\, 2\pi r dr = \text{constant} \tag{3.15}$$

The value of the constant, in order to be self-consistent with boundary conditions (3.11) and (3.12), should be taken as $-F(1 - \theta)N_{w,k}$ for $0 < z < z_F$ and $F\theta N_{p,k}$ for $z_F < z < z_H$. We first proceed to the analysis of the section $Z_F < Z < Z_H$ for which Eq. (3.15) is written

$$\int_0^a \phi_{k,z} 2\pi r dr = F\theta N_{p,k} \tag{3.16}$$

substituting Eq. (3.6) into Eq. (3.16) results in

$$F\theta N_{p,k} = A^* - B^* \tag{3.17a}$$

$$A^* = \int_0^a \rho V_z N_k 2\pi r dr \tag{3.17b}$$

$$B^* = 2\pi\rho D \int_0^a \frac{\partial N_k}{\partial Z} r dr \tag{3.17c}$$

The integral B^* is approximated very simply:

$$B^* = \pi a^2 \rho D \frac{d\overline{N}_k}{dZ} \tag{3.18}$$

The integral A^* is more complex to calculate. First, we proceed to an integration by parts by introducing the stream function Ψ defined by

$$\frac{\partial \Psi}{\partial r} = \rho r V_z \qquad \text{or} \qquad \Psi = \int_0^r \rho V_z r' dr'$$

Then we have

$$A^* = 2\pi \int_0^a N_k \frac{\partial \Psi}{\partial r} dr = 2\pi \left[N_k \Psi\right]_0^a - \int_0^a 2\pi \Psi \frac{\partial N_k}{\partial r} dr \tag{3.19}$$

In the first term on the RHS of Eq. (3.19), $2\pi\Psi(a)$ is the net transport of the mixture, i.e., $F\theta$, and N_k $(r = a)$ is approximated by $\overline{N}_k$. So we have

$$A^* = F\theta\overline{N}_k - 2\pi \int_0^a \Psi \frac{\partial N_k}{\partial r} dr \tag{3.20}$$

The transverse concentration gradient in the last term of Eq. (3.20) is estimated directly from the diffusion equation (3.8). The diffusion term $-\rho D(\partial^2 N_k/\partial Z^2)$ is disregarded and the term $\partial N_k/\partial Z$ is approximated by $d\overline{N}_k/dZ$ which is independent of r. Thus, the relationship between the transverse gradient and the axial concentration gradient takes the following form:

$$-\rho D \frac{1}{r} \frac{\partial}{\partial r} \left\{ r \frac{\partial N_k}{\partial r} - \frac{\Omega^2 r^2}{RT} N_k \left(M_k - \sum_{j=1}^{n} M_j N_j \right) \right\} + \rho V_z \frac{d\overline{N}_k}{dZ} = 0$$

Multiplying both sides by rdr and integrating from 0 to r yields

$$\frac{\partial N_k}{\partial r} = \frac{\Omega^2 r}{RT} N_k \left(M_k - \sum_{j=1}^{n} M_j N_j \right) + \frac{1}{\rho D} \frac{\Psi}{r} \frac{d\overline{N}_k}{dZ}$$

In the first term on the RHS, we approximate all the N by $\overline{N}$, and the final expression for the transverse gradient follows:

$$\frac{\partial N_k}{\partial r} = \frac{\Omega^2 r}{RT} \overline{N}_k \left(M_k - \sum_{j=1}^{n} M_j \overline{N}_j \right) + \frac{1}{\rho D} \frac{\Psi}{r} \frac{d\overline{N}_k}{dZ} \tag{3.21}$$

Substituting Eq. (3.21) into Eq. (3.20) results in

$$A^* = F\theta\overline{N}_k + \left(\frac{2\pi\Omega^2}{RT}\int_0^a \Psi r dr\right)\overline{N}_k\left(\sum_{j=1}^{n} M_j\overline{N}_j - M_k\right) - \left(\frac{2\pi}{\rho D}\int_0^a \frac{\Psi^2}{r}dr\right)\frac{d\overline{N}_k}{dZ} \tag{3.22}$$

Finally, inserting Eqs. (3.22) and (3.18) into Eq. (3.17) results in the differential equation for $\overline{N}_k$ in the enricher ($Z_F < Z < Z_H$):

$$F\theta N_{p,k} = F\theta\overline{N}_k + \left(\frac{2\pi\Omega^2}{RT}\int_0^a \Psi r dr\right)\overline{N}_k\left(\sum_{j=1}^{n} M_j\overline{N}_j - M_k\right) - \left(\pi a^2\rho D + \frac{2\pi}{\rho D}\int_0^a \frac{\Psi^2}{r}dr\right)\frac{d\overline{N}_k}{dZ} \tag{3.23}$$

With the boundary conditions

$$Z = Z_H, \qquad \overline{N}_k = N_{p,k} \tag{3.24}$$

$$Z = Z_F, \qquad \overline{N}_k = N_{0,k} \tag{3.25}$$

In Eq. (3.25) $N_{0,k}$ is an auxiliary variable which will be determined later. The differential equations for $\overline{N}_k$ in the stripper ($0 < Z < Z_F$) are obtained by changing $F\theta$ with $-F(1-\theta)$ and $N_{p,k}$ with $N_{w,k}$:

$$-F(1-\theta)N_{w,k} = -F(1-\theta)\overline{N}_k + \left(\frac{2\pi\Omega^2}{RT}\int_0^a \Psi r dr\right)\overline{N}_k\left(\sum_{j=1}^{n} M_j\overline{N}_j - M_k\right) - \left(\pi a^2\rho D + \frac{2\pi}{\rho D}\int_0^a \frac{\Psi^2}{r}dr\right)\frac{d\overline{N}_k}{dZ} \tag{3.26}$$

and in the boundary conditions

$$z = 0, \qquad \overline{N}_k = N_{w,k} \tag{3.27}$$

$$z = z_F, \qquad \overline{N}_k = N_{0,k} \tag{3.28}$$

The auxiliary variable $N_{0,k}$ should be determined from the overall balance equation for the isotope k:

$$N_{F,k} = \theta N_{p,k} + (1-\theta)N_{w,k} \tag{3.29}$$

Finally we recall that

$$\sum_{j=1}^{n} \overline{N}_j = 1 \tag{3.30}$$

Equations (3.23) to (3.30) determine the axial separation of all the isotopes in the centrifuge.

3.3. Separation Equations in Terms of Onsager's Master Potential

The set of Equations (3.23) to (3.30) is nondimensionalized and expressed in terms of Onsager's master potential by the following change of variables:

$$\begin{cases} x = A^2\left(1 - \dfrac{r^2}{a^2}\right); \qquad y = z/a; \qquad \Psi = -2A^2\rho_w\Omega a^3\chi_x \\ \varphi_p = F\theta/\pi a\rho D; \qquad \varphi_w = F(1-\theta)/\pi a\rho D; \qquad y_H = z_H/a; \qquad y_F = z_F/a \end{cases} \tag{3.31}$$

For the sake of notation simplicity, we drop from now on the overbar on the radially averaged mole fractions $\overline{N}_k$. The final set of equations governing the separation of all the isotopes in the gas centrifuge can be written:

Enricher: $y_F \leq y \leq y_H$

$$\varphi_p(N_{p,k} - N_k) = E_k N_k - h\frac{dN_k}{dy} \tag{3.32}$$

With the boundary conditions:

$$\begin{cases} y = y_H, & N_k = N_{p,k} \\ y = y_F, & N_k = N_{0,k} \end{cases} \tag{3.33}$$

$N_{0,k}$ is an auxiliary variable which will be determined later. The expressions of E_k and h are given below after the equations for the stripper.

Stripper: $0 \leq y \leq Y_f$

$$-\varphi_w(N_{w,k} - N_k) = E_k N_k - h\frac{dN_k}{dy} \tag{3.34}$$

Boundary conditions:

$$\begin{cases} \text{at} \quad y = 0, & N_k = N_{w,k} \\ \text{at} \quad y = y_f, & N_k = N_{0,k} \end{cases} \tag{3.35}$$

$$E_k = 4\mathrm{ReSc}A^2\Delta\chi\frac{\delta M_k}{M}, \qquad h = 1 + 4\mathrm{Re}^2\mathrm{Sc}^2A^2\int_0^{A^2}(\chi_x)^2dx \tag{3.36}$$

In Eq. (3.36), Re is the Reynolds number introduced in Section 2, Sc the Schmidt number Sc = $\mu/\rho D$, and $\Delta\chi$ is the radial drop of the master potential across the layer

$$\Delta\chi = \chi(x = 0, y) - \chi(x = x_T, y) \tag{3.37}$$

δM_k is dependent on all the N_j:

$$\delta M_k = \sum_{j=1}^{n} M_j N_j - M_k \tag{3.38}$$

Notice that E_k and h are different for enricher and stripper because the master potential is different for the two sections through the feed drive. Notice also that Eqs. (3.32) and (3.34) are nonlinear through δM_k in E_k. Finally, we want to point out the direct physical meaning of the master potential whose drop characterizes the transfer coefficient E_k. We recall that $N_{0,k}$ is determined from the balance equation (3.29) and that all the N_j solutions of Eqs. (3.32) to (3.38) should satisfy Eq. (3.30).

Note: The master potential terms

$$\Delta\chi \quad \text{and} \quad \int_0^{A^2} \chi_x^2 d\chi$$

involved in Eq. (3.36) are related to the separation parameters m and e_F, defined by Hoglund et al. (18) as follows:

$$m = 2\text{Re}\cdot\text{Sc}\cdot A\cdot\left[\int_0^{A^2} \chi_x^2 dx\right]^{1/2}; \qquad e_F = \frac{2\Delta\chi^2}{A^2 \int_0^{A^2} \chi_x^2 d\chi} \tag{3.39}$$

The nondimensional transfer coefficient E_k and the HETP (height of equivalent theoretical plate) h in Eq. (3.36) can also be expressed in terms of m and e_F:

$$E_k = m\sqrt{2e_F}A^2 \frac{\delta M_k}{M}; \qquad h = 1 + m^2 \tag{3.40}$$

3.4. Solution by the Iteration Method

The nonlinear set of Eqs. (3.32) to (3.38) can be solved by the iteration method used by Harink-Snijders (22). Equations (3.32) and (3.34), being nonlinear because of the term E_k, the method of iteration consists in considering, for the $(i + 1)$th iteration step, the value of E_k calculated with

all the concentrations of the ith step. Then, the set of equations for $N_{k,i+1}$ turns out to be linear:

$$\begin{cases} y_F \le y \le y_H & \varphi_P(N_{P,k,i+1} - N_{k,i+1}) = E_{k,i}N_{k,i+1} - h\dfrac{dN_{k,i+1}}{dY} \\ & y = y_H N_{k,i+1} = N_{p,k,i+1}; \quad y = y_F; \quad N_{k,i+1} = N_{0,k,i+1} \\ 0 \le y \le y_F & -\varphi_w(N_{w,k,i+1} - N_{k,i+1}) = E_{k,i}N_{k,i+1} - h\dfrac{dN_{k,i+1}}{dY} \\ & y = 0; \; N_{k,i+1} = N_{w,k,i+1}; \qquad y = y_F N_{k,i+1} = N_{0,k,i+1} \\ \text{with} & E_{k,i} = 4\mathrm{Re}\cdot\mathrm{Sc}\cdot A^2\cdot\frac{1}{M}\cdot\Delta\chi\cdot\left[\sum_{j=1}^{n} M_j N_j, i - M_k\right] \end{cases} \tag{3.41}$$

At each iteration step, the auxiliary variable $N_{0,k,i+1}$ is determined by the balance equation

$$N_{F,k} = \theta N_{p,k,i+1} + (1 - \theta)N_{w,k,i+1} \tag{3.42}$$

The solution of Eqs. (4.1) and (4.2) is straightforward. We give below the axial distribution $N_{k,i+1}(y)$ of the concentrations along the centrifuge and the end concentrations $N_{p,k,i+1}$ and $N_{w,k,i+1}$.

$0 \le y \le y_F$:

$$\frac{N_{k,i+1}(y)}{N_{F,k}} = \frac{\varphi_P + \varphi_w}{\varphi_P f_{P,k,i} + \varphi_w f_{w,k,i}} f_{w,k,i} \exp[G_{k,i}(y)]$$

$$\times \left\{1 + \varphi_w \int_0^y \frac{1}{h} \exp[-G_{k,i}(t)]dt\right\}$$

$y_F < y \le y_H$:

$$\frac{N_{k,i+1}(y)}{N_{F,k}} = \frac{\varphi_P + \varphi_w}{\varphi_P f_{p,k,i} + \varphi_w f_{w,k,i}} \exp[F_{k,i}(y)]$$

$$\times \left\{1 - \varphi_P f_{p,k,i} \int_{Y_F}^{Y} \frac{\exp[-F_{k,i}(t)]}{h}\, dt\right\}$$

$$F_{k,i}(y) = \int_{Y_F}^{Y} \frac{\varphi_P + E_{k,i}}{h}\, dt; \qquad G_{k,i}(y) = \int_0^Y \frac{-\varphi_w + E_{k,i}}{h}\, dt$$

$$f_{p,k,i} = \frac{1}{\exp[-F_{k,i}(Y_H)] + \varphi_P \displaystyle\int_{Y_F}^{Y_H} \frac{\exp[-F_{k,i}(y)]}{h}\, dy} \tag{3.43}$$

$$f_{w,k,i} = \frac{1}{\exp[G_{k,i}(Y_F)]\left\{1 + \varphi_w \int_0^{Y_F} \frac{\exp[-G_{k,i}(y)]}{h}\, dy\right\}}$$

$$\frac{N_{P,k,i+1}}{N_{F,k}} = \frac{f_{P,k,i}(\varphi_P + \varphi_w)}{\varphi_P f_{P,k,i} + \varphi_w f_{w,k,i}}; \qquad \frac{N_{w,k,i+1}}{N_{F,k}} = \frac{f_{w,k,i}(\varphi_P + \varphi_w)}{\varphi_P f_{P,k,i} + \varphi_w f_{w,k,i}}$$

At each iteration step, not only the end concentrations but also the whole axial profiles of the concentrations of *all* of the isotopes should be calculated and inserted in the expression of $E_{k,i}$ (last equation of Eqs. 3.41) in order to provide the function $E_k(y)$ to be used in the next iteration step. Note also that we should calculate the sum of the product and waste concentrations $\sum_{j=1}^{n} N_{p,j,i}$ and $\sum_{j=1}^{n} N_{w,j,i}$ at each iteration step and stop the iteration procedure when the two relations

$$\sum_{j=1}^{n} N_{p,j,i} = 1; \qquad \sum_{j=1}^{n} N_{w,j,i} = 1$$

are satisfied with a prespecified accuracy. The iteration procedure may be started by using the feed concentrations of all the isotopes.

4. OPTIMIZATION OF CENTRIFUGE PARAMETERS FOR MULTI-ISOTOPE SEPARATION AND EXAMPLES OF APPLICATION

In this section we develop a strategy for optimizing the centrifuge parameters in the case of multi-isotope separation (Section 4.1). Then we present two examples of application pertaining respectively to the reenrichment of spent reactor uranium (Section 4.2) and to the separation of the stable isotope of chromium (Section 4.3).

4.1. An Optimization Strategy for Multi-Isotope Separation

One of the end results expected from computational work on centrifugation is to predict some "optimal" centrifuge parameters. What does the term "optimal" mean? A well-posed optimization problem includes three well-specified sets of data.

a) Device and process gas data. These are the technological data of the centrifuge including the length, diameter, and peripheral speed; the process gas mixture and its properties; the feed composition of all the isotopes; the average gas temperature; and the mass holdup (or alternatively the gas pressure at the wall).

b) Controllable variables, i.e., the variables on which an external action is possible and that can be modified by the experimentor. The four countercurrent driving parameters belonging to this category are the scoop drag, the wall temperature gradient, the feed rate, and the cut. In fact, due to the linear nature of Onsager's pancake model, the countercurrent flow results from a linear combination of the four drives, each drive being calculated separately for some unitary value. We choose 1000 dynes for the angular momentum sink for the scoop drive, a difference of 1 kelvin for end-to-end temperature of wall thermal drive, and a feed of 1 kg/s for each of the upper section and lower section drives. Each of the corresponding unitary solutions of Onsager's equation is multiplied by a weight coefficient and then combined linearly. These drive weights are the controllable variables.

c) "Cost function," i.e., some quantity to optimize by determining properly the controllable variables. In the case of a binary mixture, the "cost function" is quite naturally the separative power. But in the case of a multi-isotope mixture, the separative power is no longer available. We choose the following strategy:

- We focus on one *desired isotope*.
- In addition to the device and process gas data mentioned above in a), we specify the product and waste concentrations of the desired isotope. The cut will result from this choice and the data of the feed composition through the balance equation.
- We look for the maximum value of the feed rate yielding the above fixed outlet concentrations.
- The controllable variables which will be used for optimization are two drives (scoop drive and linear wall temperature drive).

Practically we proceed by interpolation as follows. We select one nominal value of the feed rate and optimize the scoop drag and the linear wall temperature gradient to produce the largest product concentration of the desired isotope. If the resulting optimized product concentration is less than what is required, select a smaller value of the feed rate and reoptimize. But if the resulting optimized product concentration is more than the desired value, select a larger value of feed rate and reoptimize on the scoop drag and linear wall temperature gradient. This process can continue until the calculated value of the product concentration of the desired isotope is close enough to the required value. For the latter value, the waste concentration requirement is automatically satisfied because of the fixed value of the cut.

A code, operating on a PC, was created by one of us (Thomas C. Mason) to compute Onsager's equation for multi-isotope mixtures and to optimize centrifuge parameters according to the above-developed strategy. The optimization uses a quasi-Newton algorithm for finding a minimum of a function subject to fixed upper and lower bounds on the variables. The algorithm was written by Gill et al. (24) and is part of the NAG library. That code was used to carry out practical calculations in two cases, and the results are presented in the next two subsections.

4.2. Reenrichment of Spent Reactor Uranium

The device and process gas data are displayed in Table 1. The centrifuge data pertain to a test case specified during a workshop held in Darmstadt, Germany, 1987 (the *Proceedings* of this workshop are quoted in Ref. 9). The physicochemical properties of UF_6 are drawn from DeWitt (25). The additional requirements follow:

- Desired isotope: U-235
- Product concentration of the desired isotope: 3%
- Waste concentration of the desired isotope: 0.3%

The cut resulting from the specification of the U-235 concentrations in

TABLE 1
Reenrichment of Spent Reactor Uranium: Centrifuge and Process Gas Data

Length of the centrifuge	15 m
Diameter of the centrifuge	0.5 m
Peripheral speed	800 m/s
Process gas	UF_6
Average gas temperature	340 K
Gas pressure at the wall	500 torr
Molecular weight	352 g/mol
Viscosity	1.96×10^{-5} kg/m·s
Heat capacity	384 J/kg·K
Thermal conductivity	0.00782 W/m·K
Ratio of specific heats	1.065
Schmidt number	0.8
Isotopic composition of the feed:	
U-232 10^{-9}%	
U-234 0.02%	
U-235 0.9%	
U-236 0.4%	
U-238 98.68%	

the feed, product, and waste is 0.2222. The application of the optimization procedure described in Section 4.1 results in Fig. 5 where we have plotted the optimal product concentration of U-235 versus feed rate. Interpolating from this curve, it is determined that the largest feed rate satisfying the above requirements is $F_{\max} = 18.60$ mg/s and the pertaining optimal results are summarized in Table 2. Some other results pertaining to the optimum are depicted in Figs. 6 to 8. Figure 6 is the streamlines corresponding to the superposition of the four optimal drives. Figure 7 plots the two Cohen's parameters e_F (flow profile efficiency) and m (normalized countercurrent flow). Figure 8 gives the axial profiles of the concentrations of the four isotopes, U-232, U-234, U-235, and U-236 (the profile of U-238 is not plotted and can be easily derived as the difference between 1 and the sum of the four plotted profiles). Here are some comments on the results:

- The feed point is located at the midplane of the centrifuge. The scoop is located at $x = 6$, $y = 0.25$. The wall thermal drive is due to a very

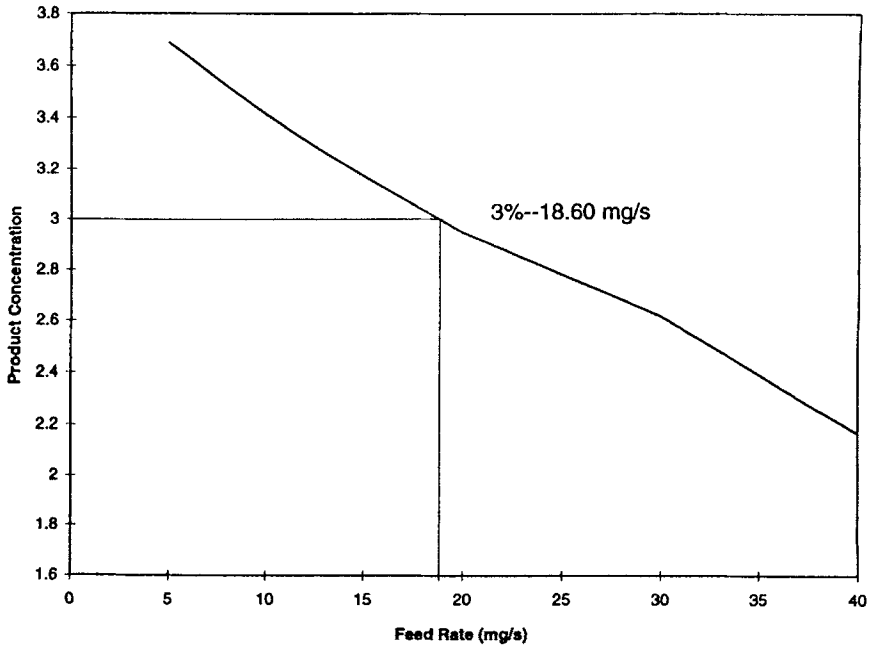

FIG. 5 Reenrichment of spent reactor uranium: Optimal product concentration of U-235 versus feed rate for the cut $\theta = 0.2222$.

TABLE 2
Reenrichment of Spent Reactor Uranium: Results of Optimization

Optimal countercurrent:	
Feed rate	18.60 mg/s
Cut	0.2222
Scoop drag	1290 dynes
End-to-end temperature difference	0.902 K

Isotopic composition of the product and of the waste:

Isotope	Product concentration (%)	Waste concentration (%)
U-232	0.43360×10^{-8}	0.46974×10^{-10}
U-234	0.077345	0.0036179
U-235	3.0039	0.29895
U-236	1.0270	0.22087
U-238	95.893	99.476

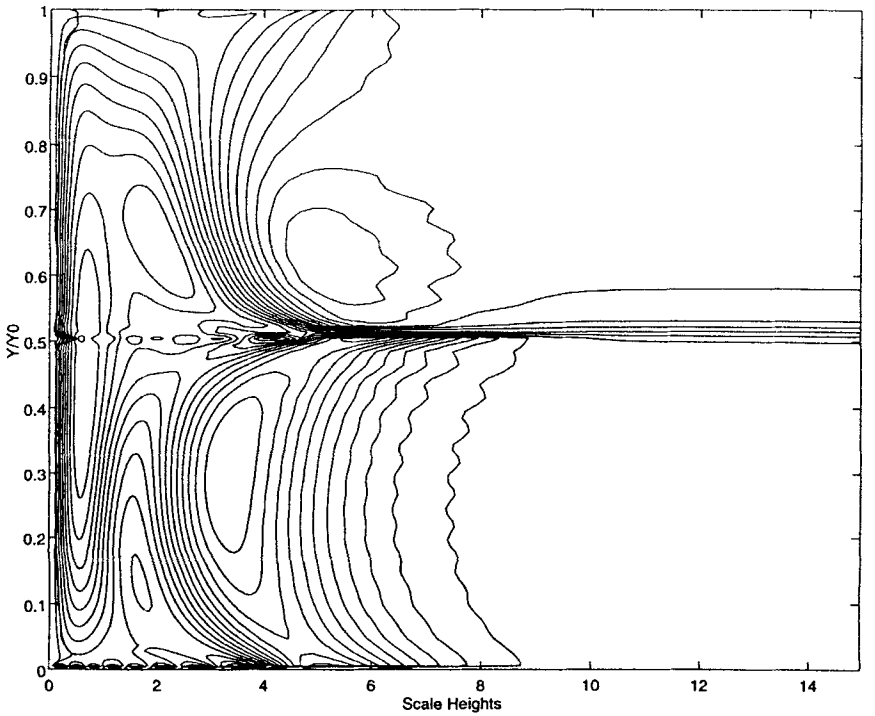

FIG. 6 Reenrichment of spent reactor uranium: Streamlines for the optimal centrifuge parameters.

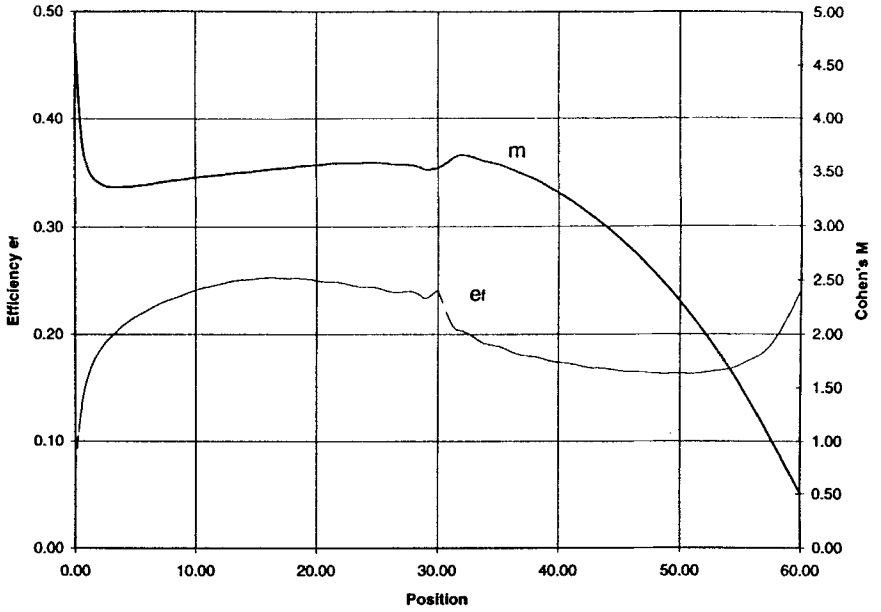

FIG. 7 Reenrichment of spent reactor uranium: Flow profile efficiency e_F and scaled countercurrent flow m for the optimal centrifuge parameters.

small gradient of temperature. The optimal temperature profile on the boundaries (caps and side wall) is very close to isothermal.

- The reenrichment of spent reactor uranium to 3% of U-235 can be achieved in a single stage cascade by the centrifuge defined in Table 1. Due to technology progress, such a centrifuge does not seem to be unimaginable.
- There is an important presence of U-236 in the product flow (about 1%). As this isotope is neutron absorbing, it will be advisable to reenrich the spent reactor uranium to a concentration of U-235 slightly greater than the usual 3% reactor grade.
- The enrichment factor of U-232 is the highest (about 4.3). Nevertheless, as this isotope is in small proportion in the feed, it will remain in reasonable proportion in the product.

4.3. Enrichment of Chromium 50

The second example of application involves the enrichment of chromium 50 from a naturally occurring 4 isotope mixture. Szady (2), using

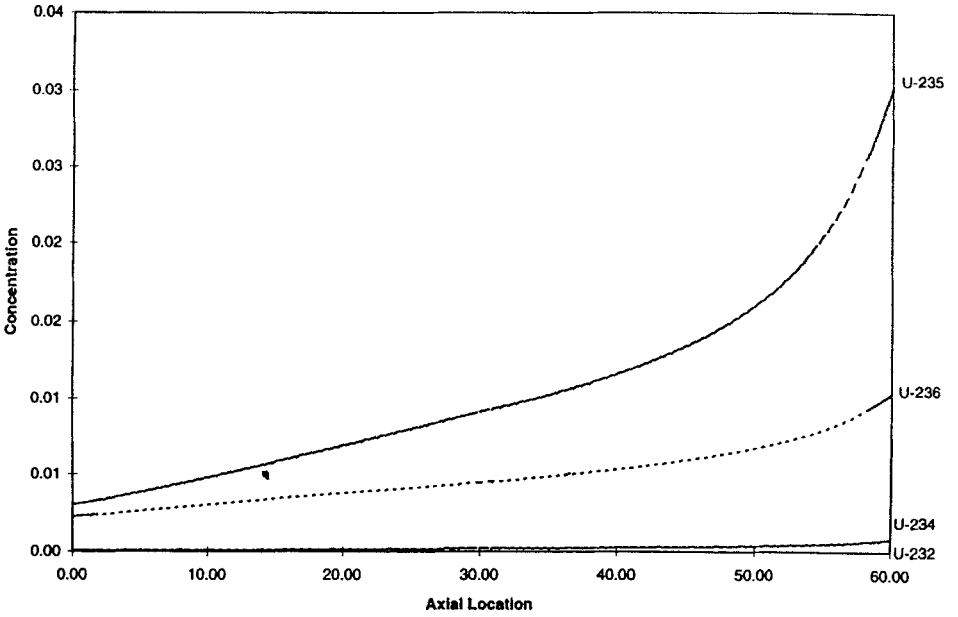

FIG. 8 Reenrichment of spent reactor uranium: Axial profiles of the concentrations of the isotopes for the optimal centrifuge parameters.

centrifugation facilities at Oak Ridge, was able to obtain 16.2% Cr-50 product using 4.35% Cr-50 feed with a waste of 3% Cr-50. The device and process gas data are listed in Table 3. The physicochemical properties of CrO_2F_2 are due to the courtesy of Borisevich (26). The additional requirements follow:

- Desired isotope: Cr-50
- Product concentration of the desired isotope: 16.2%
- Waste concentration of the desired isotope: 3.0%

The cut resulting is calculated to be 0.10227. The application of the optimization procedure results in Fig. 9 where we have plotted the optimal product concentration of Cr-50 as a function of the feed rate. Interpolation from this curve determines the largest feed rate to yield the desired concentration to be 50 mg/s. The optimal results are summarized in Table 4. The product and waste concentrations obtained experimentally by Szady are also listed in Table 4 for comparison with the computed results. The results seem to be very close, but the agreement should be considered

TABLE 3
Separation of Chromium Isotopes: Centrifuge and Process Gas Data

Length of the centrifuge	15 m
Diameter of the centrifuge	0.5 m
Peripheral speed	800 m/s
Process gas	CrO_2F_2
Average gas temperature	315 K
Gas pressure at the wall	50 torr
Molecular weight	122 g/mol
Viscosity	1.40×10^{-5} kg/m·s
Heat capacity	636 J/kg·k
Thermal conductivity	0.00675 W/m·k
Ratio of specific heats	1.12
Schmidt number	0.75
Isotopic composition of the feed:	
Cr-50 4.35%	
Cr-52 83.79%	
Cr-53 9.50%	
Cr-54 2.36%	

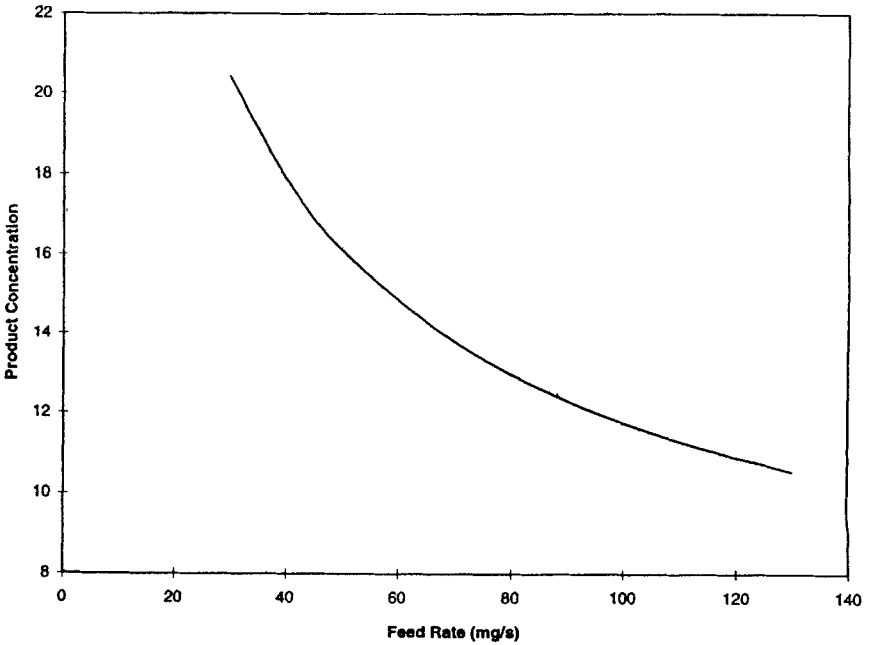

FIG. 9 Enrichment of chromium-50: Optimal product concentration of Cr-50 versus feed rate for the cut $\theta = 0.10227$.

TABLE 4
Separation of Chromium Isotopes: Results of Optimization

Optimal countercurrent	
Feed rate	50 mg/s
Cut	0.10227
Scoop drag	5512 dynes
End-to-end temperature difference	5.66 K

Isotopic composition of the product and of the waste:

Isotope	Product-Szady[a] (%)	Product-Code[b] (%)	Waste-Szady[a] (%)	Waste-Code[b] (%)
Cr-50	16.2	16.122	3.0	3.009
Cr-52	79.4	79.715	84.3	84.254
Cr-53	4.0	3.789	10.1	10.150
Cr-54	0.4	0.373	2.6	2.586

[a] Product-Szady, Waste-Szady: Experimental results from Ref. 2.
[b] Product-Code, Waste-Code: Computed results by our code.

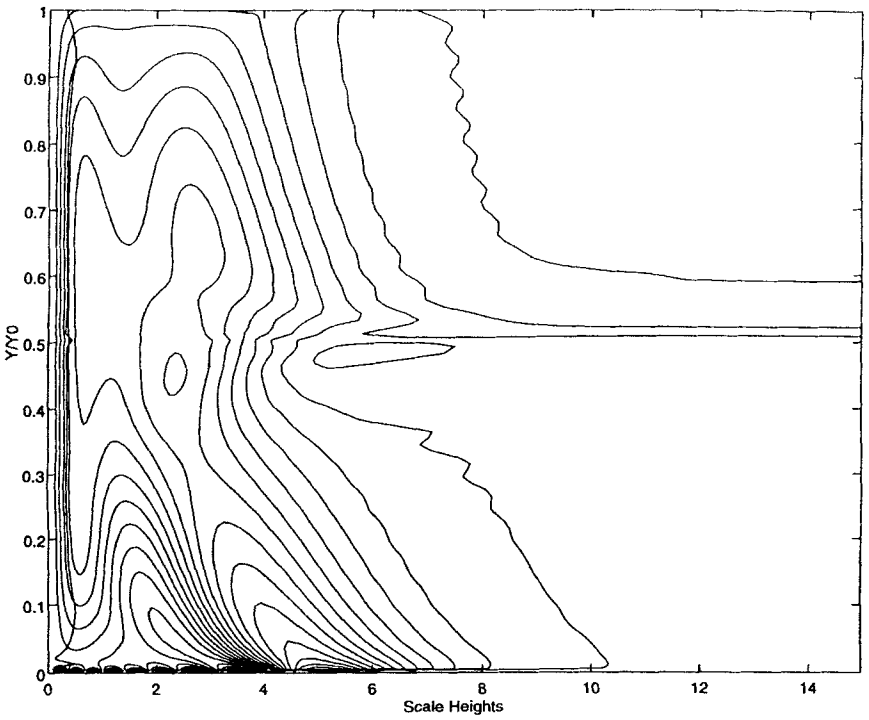

FIG. 10 Enrichment of chromium-50: Streamlines for the optimal centrifuge parameters.

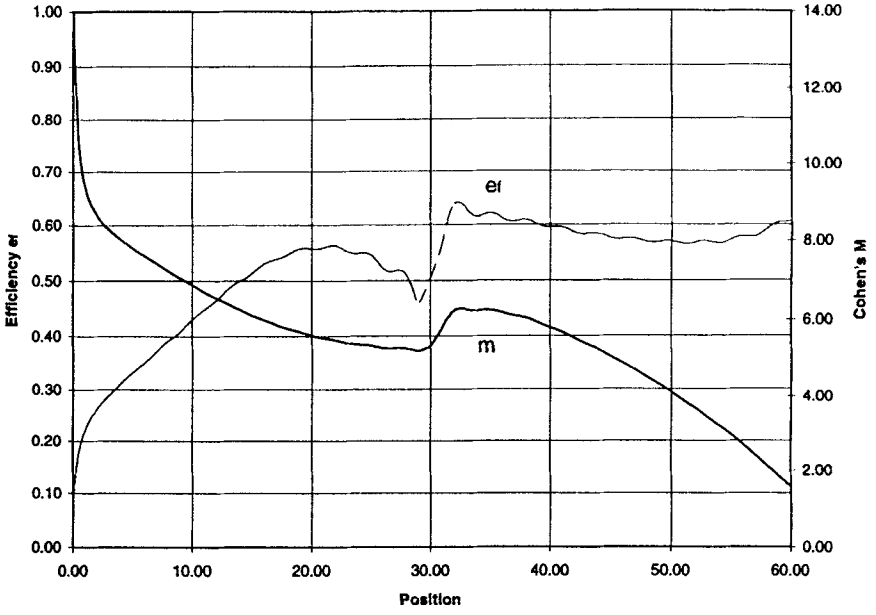

FIG. 11 Enrichment of chromium-50: Flow profile efficiency e_F and scaled countercurrent flow m for the optimal centrifuge parameter.

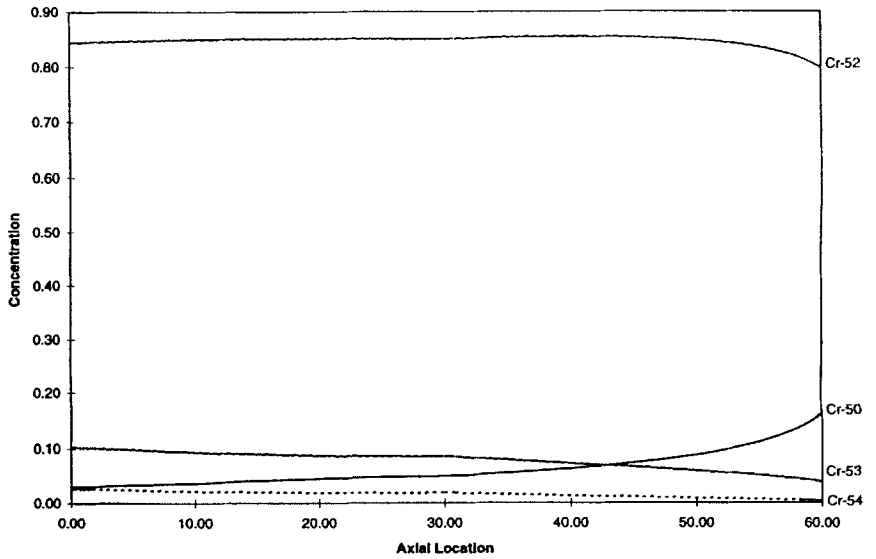

FIG. 12 Enrichment of chromium-50: Axial profiles of the concentrations of the isotopes for the optimal centrifuge parameters.

only as a qualitative comparison as the physical parameters of the centrifuge used by Szady are not published. Further results of our optimization computations include a stream functions plot (Fig. 10), a plot of Cohen's parameters m and e_F (Fig. 11) and a plot of the concentration axial profiles of the four isotopes (Fig. 12).

5. CONCLUSIONS

A method to compute the optimal multi-isotope separation in a gas centrifuge is developed in this article. The method relies on three models:

- Onsager's pancake model to solve for the countercurrent flow.
- Radial averaged diffusion equations to solve for the concentrations of all the isotopes (solution by iteration method).
- Optimization methodology to compute the optimal countercurrent drive parameters.

The method works with very light computing equipment. As a practical application of the method, we have calculated the reenrichment of spent reactor uranium with a long and high speed centrifuge permitting the enrichment to reactor grade in a single-stage cascade. But the method can be extended to short and lower speed centrifuges. In the latter case the calculations should be completed by an appropriate cascade calculation. A second practical computation was also carried out in one case of stable isotope production. The enrichment of chromium-50 was calculated, but the model can easily be applied to any stable isotope separable by centrifugation.

REFERENCES

1. W. L. Roberts, "Gas Centrifugation of Research Isotopes," *Nucl. Instrum. Methods Phys. Res., A282*, 271–276 (1989).
2. A. J. Szady, "Enrichment of Chromium Isotopes by Gas Centrifugation," *Ibid., A282*, 277–280 (1989).
3. C. Ying and Z. Guo, "Some Characteristics for Multicomponent Isotope Separation," in *Proceedings of the Fourth Workshop on Separation Phenomena in Liquids and Gases* (C. Ying, Ed.), Tsinghua University, Beijing, China, 1995.
4. V. D. Borisevich, G. A. Potapov, G. A. Sulaberidze, and V. A. Chuzhinov, "Multicomponent Isotope Separation in Cascades with Additional External Flows," in *Proceedings of the Fourth Workshop on Separation Phenomena in Liquids and Gases* (C. Ying, Ed.), Tsinghua University, Beijing, China, 1995.
5. V. E. Fillippov and L. Y. Sosnin, "Modelling of Gas Flow and Separation Process of Multicomponent Mixture of Isotopes in Countercurrent Centrifuge with Internal Input of Feed," in *Proceedings of the Fourth Workshop on Separation Phenomena in Liquids and Gases* (C. Ying, Ed.), Tsinghua University, Beijing, China, 1995.
6. V. D. Borisevich, E. V. Levin, S. V. Yupatov, and E. M. Aisen, "Numerical Investiga-

tion of the Separation of Sulfur Isotopes in a Single Gas Centrifuge," *At. Energy*, *76*(6), 454–458 (1994).
7. E. Rätz, E. Coester, and P. deJong, "Production of Stable Isotopes by Gas Centrifuge," in *Proceedings of the International Symposium on Synthesis and Applications of Isotopes and Isotopically Labelled Compounds*, Toronto, 1991.
8. R. C. Raichura, M. A. M. Al-Janabi, and G. M. Langbein, "Some Aspects of the Separation of Multi-Isotope Mixtures with Gas Centrifuges," in *Proceedings of the Second Workshop on Separation Phenomena in Liquids and Gases* (P. Louvet et al., Eds.), C.E.A. Saclay, 91191 Gif-Sur Yvette Cedex, France, 1989.
9. E. Von Halle, "Multicomponent Isotope Separation in Matched Abundance Ratio Cascade of Stages with Large Separation Factors," in *Proceedings of the First Workshop on Separation Phenomena in Liquids and Gases* (K. Roesner, Ed.), Technische Hochschule, Darmstadt, Germany, 1987.
10. A. De La Garza, "A Generalization of the Matched Abundance-Ratio Cascade for Multicomponent Isotope Separation, *Chem. Eng. Sci.*, *18*, 73–82 (1963).
11. A. De La Garza, G. A. Garrett, and J. E. Murphy, "Multicomponent Isotope Separation in Cascades," *Ibid.*, *15*, 188–209 (1961).
12. I. Yamamoto and A. Kanagawa, "Synthesis of Value Function for Multicomponent Isotope Separation, *Nucl. Sci. Technol.*, *16*(1), 43–48 (1979).
13. Y. Lehrer-ilamed, "On the Value Function for Multicomponent Isotope Separation," *Nucl. Technol.*, *23*, 559–567 (1969).
14. H. G. Wood and J. B. Morton, "Onsager Pancake Approximation for the Fluid Dynamics of a Gas Centrifuge," *J. Fluid Mech.*, *101*, 1–31 (1980).
15. H. G. Wood and G. Sanders, "Rotating Compressible Flows with Internal Sources and Sinks," *Ibid.*, *127*, 299–313 (1983).
16. H. G. Wood and R. Babarsky, "Analysis of a Rapidly Rotating Gas in a Pie-Shaped Cylinder," *Ibid.*, *239*, 249–271 (1992).
17. H. G. Wood, "Analysis of Feed Effects on a Single Stage Gas Centrifuge Cascade," *Sep. Sci. Technol. 30*(13), 2631–2657 (1995).
18. R. L. Hoglund, J. Shacter, and E. Von Halle, "Diffusion Separation Methods," in *Encyclopedia of Chemical Technology*, Vol. 7, 3rd ed. (R. E. Kirk and D. F. Othmer, Eds.), Wiley, New York, 1979.
19. E. Von Halle, "The Countercurrent Gas Centrifuge for the Enrichment of U-235," in *Proceedings 70th Annual Meeting AIChE*, AIChE, New York, 1977.
20. K. Cohen, *The Theory of Isotope Separation*, McGraw-Hill, New York, 1952.
21. Soubbaramayer, "Centrifugation," in *Uranium Enrichment* (S. Villani, Ed.), Springer-Verlag, New York, 1979.
22. H. G. M. Harink-Snijders, "Solving the Diffusion Equation for Multi-Isotope Mixtures," in *Proceedings of the Third Workshop on Separation Phenomena in Liquids and Gases* (H. G. Wood, Ed.), University of Virginia, Charlottesville, VA, USA, 1992.
23. G. R. Cooper and J. B. Morton, "Driven Wave Motions in a Rotating Gas," *J. Fluids Struct.*, *2*, 453–477 (1988).
24. P. E. Gill, W. Murray, S. M. Picken, M. H. Wright, and E. M. R. Long, *Mark 6 Release NAG*, D.N.A.C., National Physical Laboratory, England (1977).
25. R. DeWitt, *UF_6: A Survey of the Physico-Chemical Properties*, Goodyear Atomic Corp., 1960.
26. V. Borisevich, Private Communication, 1995.

Received by editor August 21, 1995